geosciences

MDPI

Article

Stability Assessment of Volcanic Lava Tubes Using Engineering Rock Mass Classifications and an Empirical Approach

Abdelmadjid Benrabah, Salvador Senent Domínguez and Luis Jorda-Bordehore *

ETSI Caminos, Canales y Puertos, Universidad Politécnica de Madrid, 28040 Madrid, Spain; abdelmadjid.benrabah@alumnos.upm.es (A.B.); s.senent@upm.es (S.S.D.)
* Correspondence: l.jorda@upm.es

Abstract

Volcanic caves, commonly referred to as lava tubes, are typically shallow subsurface cavities formed by the cooling of a generally basaltic lava flow under a roof or crust that cools faster and acts as a thermal insulator. These cavities can serve as tourist attractions, in which case their stability must be analyzed and ensured. Empirical rock mass classification systems, in this case we have applied the Q-index have been employed to evaluate the stability of underground excavations: mines and tunnels, including natural caves. We have identified that these approaches have limitations, particularly incorporating key geometric parameters such as roof thickness and cave length. In this study we have analyzed applicability of the Scaled Span Method (SSM) to volcanics caves. This method was originally developed for the stability assessment of crown pillar stability in shallow mines. We have developed a dataset of lava tubes (caves) located in the Canary Islands (Spain), the Galápagos Islands (Ecuador), and Jordan. In this research we have conducted geomechanical characterization using the Q-system, and also the Scaled Span to evaluate stability based on cave geometry and rock mass properties. The results indicate that, in general, the SSM yields more conservative stability estimates compared to the Q-system, particularly for shallow caves with limited roof thickness. Nevertheless, discrepancies between the two approaches are observed in several cases, highlighting the limitations of directly transferring empirical methods developed for mining excavations to natural cave systems. These differences underscore the need for careful interpretation and, where appropriate, complementary stability analyses. The Scaled Span Method is useful for preliminary assessment of volcanic cave stability, especially in scenarios where potential interaction with the ground surface is expected: buildings or roads on top. However, its application requires adaptation and critical evaluation due to the fundamental differences between engineered mining excavations and natural subsurface cavities.

Keywords: lava tubes; volcanic cave; q index; stability assessment; scaled span; empirical approach

Check for updates

Academic Editors: Salvatore Grasso and Pinnaduwa Kulatilake

Received: 21 April 2026
Revised: 25 June 2026
Accepted: 7 July 2026
Published: 15 July 2026

Copyright: © 2026 by the authors. Licensee MDPI, Basel, Switzerland. This article is an open access article distributed under the terms and conditions of the Creative Commons Attribution (CC BY) license.

1. Introduction

Volcanic caves, commonly known as lava tubes, are natural subsurface voids formed during the emplacement and cooling of basaltic lava flows [1]. These structures are distributed in volcanic regions such as the Canary Islands (Spain) and the Galápagos Islands (Ecuador), where they often develop at shallow depths and may extend over considerable distances [1–3]. Due to their proximity to the surface, lava tubes are particularly susceptible

to external loading conditions and may occur beneath infrastructure or within areas of touristic interest, making their stability assessment a critical geotechnical issue [1].

From a mechanical perspective, the stability of lava tubes is governed by a combination of geometric and material factors, with roof thickness and span playing a dominant role in controlling failure mechanisms. Shallow cavities are especially vulnerable, as reduced overburden thickness increases the likelihood of collapse under relatively low stress conditions. Unlike engineered underground excavations, these natural voids are not designed to withstand external loads, and their failure is often abrupt and difficult to predict. Consequently, reliable methods for stability assessment are essential for hazard evaluation, particularly in urban or infrastructure-sensitive areas [4,5].

The stability of underground openings has traditionally been evaluated using empirical rock mass classification systems, among which the Q-system is one of the most widely applied methods. This approach integrates key parameters describing rock mass quality, providing a practical framework for engineering design. Owing to its simplicity, the Q-system has also been applied to natural caves, including lava tubes [2,3]. However, its applicability to shallow subsurface cavities is limited, as it does not explicitly incorporate critical geometric variables such as roof thickness or span-to-thickness ratio, which are fundamental in controlling instability in volcanic caves [6–9]; more generally, the limitations and potential misuse of rock mass classification systems outside their original tunnelling context have been widely discussed in the international literature.

To address these limitations, alternative approaches have been proposed. The Scaled Span Method (SSM), originally developed for assessing crown pillar stability in underground mining, explicitly combines geometric and geomechanical parameters, including cavity span, overburden thickness, and a shape factor [10–12]. This method has proven effective in mining environments, particularly for shallow excavations where interaction with the ground surface is significant [10–12].

Despite its potential, the application of the Scaled Span Method to natural cave systems remains insufficiently explored [1,13]. Previous studies have suggested its usefulness for volcanic caves; however, a systematic evaluation under natural conditions is still lacking. In particular, no standardized framework exists to account for the fundamental differences between engineered excavations and naturally formed cavities, such as irregular geometries, heterogeneous rock masses, and complex discontinuity networks [1]. These limitations raise important questions regarding the direct transferability of mining-based empirical methods to volcanic cave environments [2,5].

In this context, the present study evaluates the applicability of the Scaled Span Method to volcanic caves through the analysis of a dataset of lava tubes. The results are compared with those obtained using the Q-system to assess consistency and identify potential discrepancies. The specific objectives are: (i) to calculate scaled span values based on geometric and geomechanical characteristics; (ii) to compare stability predictions derived from the SSM and the Q-system; and (iii) to identify key limitations and sources of uncertainty associated with both approaches. This work aims to contribute to the development of a more robust framework for the stability assessment of volcanic caves, particularly in shallow environments where interaction with surface conditions is critical.

2. Regional Framework, Geological Setting and Origin of Lava Tubes

2.1. Geology of the Regions Studied

Lanzarote, located in the easternmost sector of the Canary Islands (Spain), is a volcanic island formed as part of an intraplate hotspot system associated with the African Plate [14,15]. The island lies approximately 125 km off the northwestern coast of Africa and is predominantly composed of basaltic volcanic formations [16] (see Figure 1).



Figure 1. Location and geological context of the Lanzarote island and studied lava tubes.

Its geological evolution is marked by several eruptive stages, with the most recent and well-documented activity corresponding to the Timanfaya eruptions (1730–1736), followed by a later eruptive episode in 1824 [17]. These events produced extensive basaltic lava flows that cover a significant portion of the island, resulting in a relatively young volcanic landscape characterized by well-preserved surface morphologies and subsurface features [18].

The volcanic deposits are mainly basaltic and exhibit both ʻaʻā and pāhoehoe lava facies, reflecting variations in rheological properties, emplacement conditions, and cooling histories [19]. Lava tube formation is closely associated with these effusive processes, particularly in flows characterized by sustained lava supply and effective thermal insulation. Under such conditions, stable flow pathways can develop beneath a solidified crust, facilitating the formation of extensive subsurface conduits [20].

Consequently, Lanzarote hosts a wide variety of lava tubes with diverse geometries and spatial distributions. Notable examples include the Cueva de los Verdes, the Jameos del Agua, and the extensive La Corona lava tube system, which together form one of the most significant volcanic cave systems in the world. These cavities generally develop along sub-horizontal trajectories, with their dimensions controlled by factors such as lava discharge rate, cooling dynamics, and local topographic gradients [21].

Internally, their structure is influenced by cooling-induced fracturing, vesicle distribution, and pre-existing discontinuities, resulting in a heterogeneous rock mass. From a geomechanical standpoint, the relatively shallow position of many of these cavities, together with variations in roof thickness and span, plays a fundamental role in their stability [22–26]. The interaction between geometric configuration and rock mass quality governs their mechanical response, making these structures particularly suitable for analysis using empirical and semi-empirical stability assessment methods [1].

The Galápagos Archipelago represents an active hotspot-related volcanic system located in the eastern Pacific Ocean, approximately 1000 km west of mainland Ecuador. Its evolution is controlled by the movement of the Nazca Plate over a relatively stationary

mantle plume, resulting in a spatial distribution of volcanic edifices with progressively increasing age from west to east [1–3] (see Figure 2).



Figure 2. Location and geological context of the Galapagos islands.

Lava tube formation in the Galápagos is linked to extensive basaltic flows emplaced under sustained eruptive conditions, which favor the development of continuous and well-organized conduit systems. Representative examples include the lava tubes of Santa Cruz Island (e.g., Bellavista), which exhibit significant lateral continuity and locally complex internal configurations [1–3].

From a geomechanical perspective, the stability of these cavities depends on the interaction between span and roof thickness, as well as rock mass characteristics. However, the larger scale and structural complexity observed in some Galápagos lava tubes introduce additional uncertainty in stability assessment. Moreover, their shallow depth increases their sensitivity to surface loading, which may lead to collapse in certain conditions [2].

Harrat al Shaam is one of the largest intraplate volcanic provinces in the Middle East, extending across northeastern Jordan, southern Syria, and northwestern Saudi Arabia. Its evolution is associated with regional extensional tectonics linked to the Dead Sea Transform system, which has facilitated repeated basaltic magma ascent through deep crustal fractures [27–29] (see Figure 3).

Lava tubes occur within several smooth-surfaced basaltic flow units, although they are generally less extensively mapped compared to island volcanic systems. Their formation is consistent with the same fundamental processes observed in Lanzarote and the Galápagos, where insulating surface crusts develop during effusive emplacement, allowing sustained internal lava transport. Once the lava supply ceases, drainage of the molten core leads to the formation of elongated subsurface voids with sub-horizontal geometry [19,20].

A representative example is the Al-Badia lava tube system in northeastern Jordan, which preserves well-defined morphological features such as smooth internal surfaces, flow structures, and localized roof collapse zones. These characteristics are broadly consistent with those observed in volcanic caves from Lanzarote (e.g., La Corona system, Cueva de

los Verdes) and the Galápagos (e.g., Bellavista lava tubes), although differences arise in scale, preservation, and geological context [4,5].

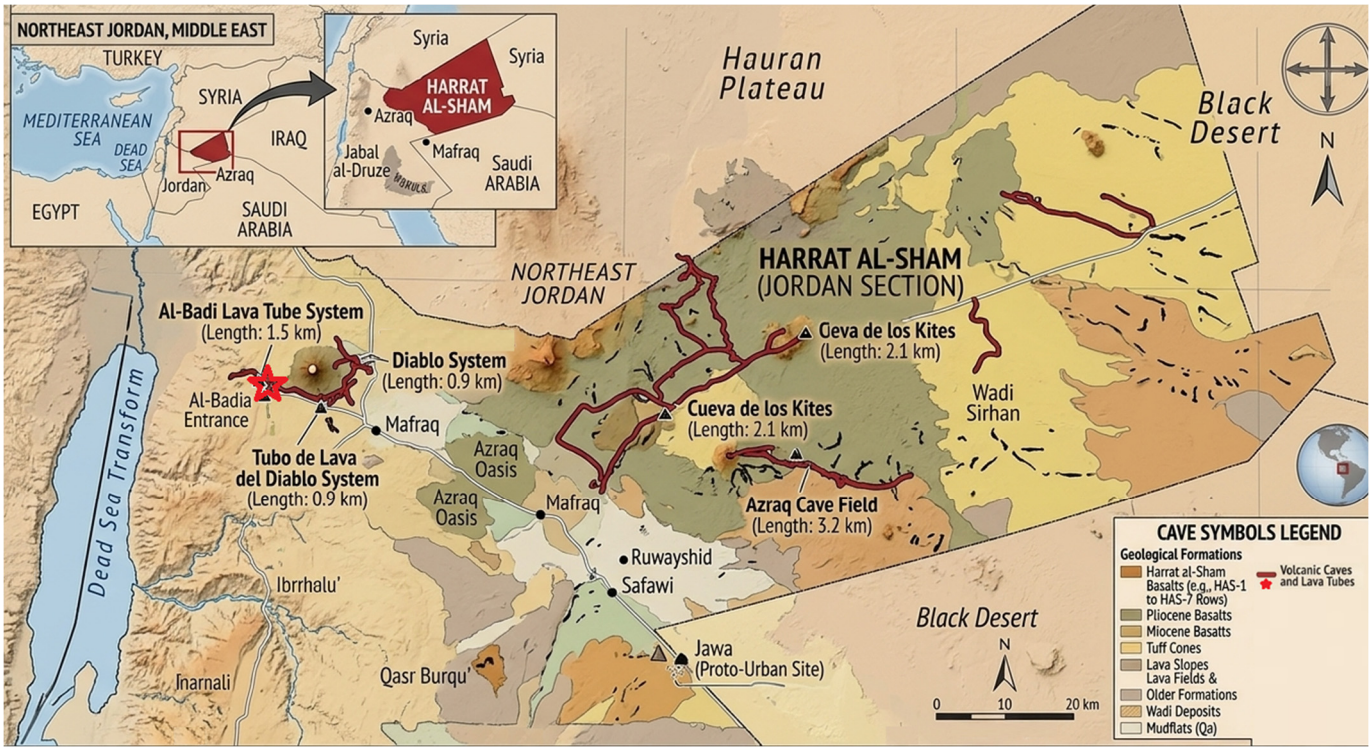

Figure 3. Location and geological referencing of the study area, the Harrat Al-Shaam lava plateau.

From a geomechanical perspective, lava tubes in Harrat al Shaam share the same primary controlling factors identified in the other studied regions, particularly roof thickness, span, and rock mass quality [30]. However, the continental setting introduces distinct boundary conditions compared to island environments. The arid climate limits chemical weathering and hydrogeological alteration, resulting in relatively well-preserved basaltic units. This contrasts with more humid volcanic settings where secondary processes may influence rock mass degradation. These climatic conditions are directly reflected in the Q-system parameters adopted in this study: dry joints (Jw = 1) and generally low joint alteration values (Ja) were recorded at all the geomechanical stations (see Table 1).

Overall, Harrat al Shaam provides a complementary continental endmember to the island-based volcanic systems of Lanzarote and the Galápagos. This combination of environments allows for a more robust assessment of empirical stability approaches under contrasting geological, climatic, and structural conditions.

2.2. Formation of Lava Tubes

Despite extensive research on volcanic systems regarding eruptive mechanisms and surface morphologies, the processes controlling the initiation and evolution of lava tubes are still not fully understood [20]. Compared to other volcanic features, the speleogenesis of lava conduits has received relatively limited attention, and several aspects of their development, geometry, and long-term stability remain topics of ongoing investigation [31].

Lava tubes originate during effusive basaltic eruptions through a combination of thermal and hydraulic processes. As lava is emplaced, the upper surface of the flow rapidly cools and solidifies upon contact with the atmosphere, forming a rigid insulating crust [21]. Beneath this layer, molten material continues to be transported within a confined pathway. When the eruption wanes or lava discharge decreases, the internal molten core may drain

partially or completely, leaving behind an empty elongated cavity with a predominantly sub-horizontal orientation. In some cases, roof failure later exposes these voids through collapse structures such as skylights or sinkholes [32] (see Figure 4).

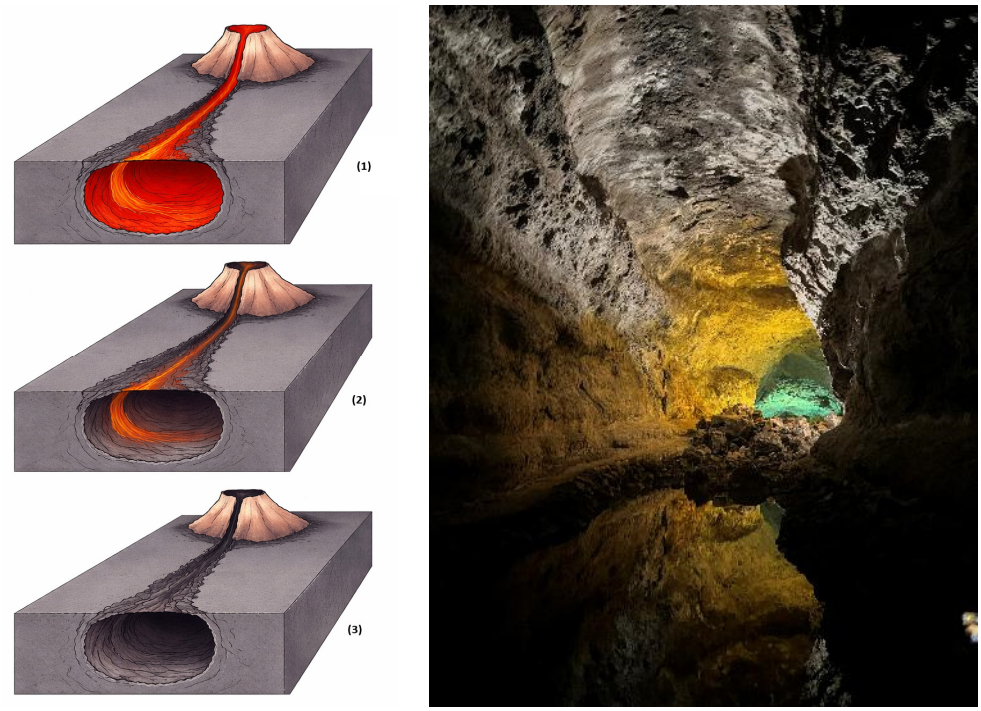

(**a**) (**b**)

Figure 4. (**a**) Conceptual model of lava tube formation. Lava flows downslope following gravity. As the surface cools and solidifies, it forms an insulating crust that keeps the molten. When the lava supply decreases, the molten core drains, leaving an empty tube. (**b**) Example of a shallow lava tube where its structure can be observed, Cueva de los Verdes, Lanzarote.

In contrast to engineered underground excavations, lava tubes develop within natural volcanic formations that generally lack pre-existing structural reinforcement. Their mechanical behavior is therefore governed by the inherent properties of the rock mass and the geometry of the cavity rather than by design considerations [22,33]. As a result, failure mechanisms are typically sudden, with limited precursory deformation, and are dominated by brittle collapse of the roof [25].

From a geotechnical perspective, lava tubes represent a relevant source of subsurface instability, particularly when located at shallow depths beneath anthropized areas [34]. Their presence can affect the performance of surface and near-surface infrastructure, including buildings, roads, and utility networks. In this sense, their behavior is comparable to other underground voids such as abandoned mine workings or karstic cavities, which are well recognized for their potential to induce ground collapse and sinkhole formation [35].

A key challenge lies in the fact that lava tubes are often not detected during preliminary site investigations and may only become apparent during excavation or construction activities. When such cavities remain unidentified, they can pose a significant hazard to overlying structures. Reported cases of sudden collapse highlight the potential severity of these failures and underscore the need for improved subsurface characterization in volcanic terrains [34].

Accordingly, the identification and assessment of lava tubes are essential components of geotechnical hazard evaluation in volcanic regions. A robust understanding of these systems requires the integration of geological observations with geometric and rock mass characterization, enabling more reliable evaluation of their stability and associated risks [1].

2.3. Characteristics of Studied Lava Caves

This study evaluates the stability of a selected set of volcanic caves located in the Canary Islands, the Galápagos Archipelago, and the Harrat al Shaam volcanic field (Jordan). From a broader inventory of lava tubes compiled by the authors during previous research campaigns in these three regions [1,4,5,13], a representative subset was selected to capture a range of geological, morphological, and geomechanical conditions.

The final dataset consists of 15 lava caves and volcanic tube systems, some of which include multiple internal stations or chambers due to their geometric complexity. The analyzed sites include well-known lava tube systems such as the Cueva de los Verdes and the Jameos del Agua (Lanzarote, Canary Islands) (Figure 5), the Mirador and Gallardo lava tubes (Santa Cruz Island, Galápagos), and the Al-Badia and Azzam lava tube system (Harrat al Shaam, Jordan).



(**a**) (**b**)

(**c**) (**d**)

Figure 5. *Cont.*



(e)



(f)

Figure 5. (**a**) The corona Volcan. (**b**) Jameo hundido. (**c**) First entrance to the Cueva de los verdes. (**d**) Second entrance to the Cueva de los verdes. (**e**) Auditorio. (**f**) Jameo del Agua.

Geomechanical field investigations were carried out at each site through the establishment of observation stations distributed along accessible sections of the caves. At each station, rock mass quality was evaluated using standard geotechnical classification parameters, while key geometric variables were recorded whenever possible, including cave height, width, and longitudinal extent. These measurements were used to characterize the overall morphology and scale of each lava tube system.

The combination of geometric and geomechanical data provides the basis for stability assessment using empirical approaches. The dataset was specifically designed to cover a wide range of structural configurations, enabling comparison between different volcanic environments and allowing assessment of the influence of geometry and rock mass quality on cave stability.

3. Materials and Methods

The methodology adopted for the assessment of cave stability combines empirical rock mass classification systems with the geometry-based Scaled Span Method. This integrated approach is widely recognized in rock engineering practice for the preliminary evaluation of underground excavations and natural cavities and provides a robust framework for characterizing both geometric and mechanical conditions of rock masses [6–8,13]. The analysis was conducted through three main stages, following the workflow adopted in previous cave-stability studies by the authors [6–8,13]:

- Fieldwork with Geotechnical Observation:

Field campaigns were carried out at each study site to collect geometric and geomechanical information. Geomechanical stations were established along accessible sections of the caves to characterize rock mass conditions and identify potential instability features.

At each station, the main discontinuity sets were identified and characterized in terms of orientation, spacing, persistence, aperture, roughness, infilling, weathering, and seepage, following standard rock mass description procedures [6–8,22,36]. Discontinuity orientations were measured with a compass–clinometer, while rock strength was estimated in situ using a Schmidt hammer to obtain indirect values of uniaxial compressive strength (UCS). A laser distance meter was employed to capture detailed geometric measurements, including cave height, width, and span.

In addition, the stability condition of each station was classified visually in the field into three categories: (i) stable, where no evidence of recent block detachment, open fracturing, or fresh debris was observed; (ii) minor instabilities, where localized block falls, open joints, or small accumulations of recent debris were identified, without compromising the overall configuration of the cavity; and (iii) unstable, where active or recent roof failures, large collapse debris cones, skylights, or propagating fracturing affecting the crown were recognized. This qualitative classification, analogous to the criteria adopted in previous studies of natural caves [6,37], was used as an independent term of comparison for the empirical methods; its inherent subjectivity and limitations are addressed in the Discussion.

- Cabinet work for determining rock mass quality indices: RMR, Q, and SSM:

Field data were complemented with office work to derive rock mass quality indices, including the Rock Mass Rating (RMR) and the Q-system. Computational analyses were also performed to determine the Scaled Span Method (SSM) using Rocscience software CPillar v5 [38].

- Discussion and comparison of results:

The results obtained from the different approaches were analyzed and compared following the outlined methodology.

3.1. Geomechanical Station and Rock Mass Classification

The stability of underground openings is commonly evaluated through empirical rock mass classification systems, among which the Q-system [23] and the Rock Mass Rating (RMR) system [22,39] are the most widely used approaches.

The Q-system, originally developed at the Norwegian Geotechnical Institute in 1974, quantifies rock mass quality by combining several geotechnical parameters into a single numerical index, where higher values correspond to better rock mass conditions [23]. The formulation of the index is given as

$$Q = \frac{RQD}{Jn} \times \frac{Jr}{Ja} \times \frac{Jw}{SRF}$$

where RQD (%) represents the Rock Quality Designation, Jn is the joint set number, Jr is the joint roughness coefficient, Ja is the joint alteration coefficient, Jw is the joint water reduction factor, and SRF is the stress reduction factor, which reflects the influence of in situ stress conditions and structural weaknesses within the rock mass.

Table 1. Q-system rock mass classification description. Adapted from [8,38].

Q Index	Definition Q Rating
0.001–0.01	Exceptionally poor
0.01–0.1	Extremely poor
0.1–1	Very poor
1–4	Poor
4–10	Fair
10–40	Good
40–100	Very Good

The Rock Mass Rating (RMR) system, originally introduced by Bieniawski in 1973, is a geomechanical classification method used to evaluate rock mass quality and to estimate the stability and support requirements of underground excavations. It has been widely adopted in both engineering and geological applications.

The RMR system is based on the summation of several weighted parameters that describe the condition and behavior of a rock mass. These include the uniaxial compressive

strength (UCS) of intact rock, Rock Quality Designation (RQD), spacing of discontinuities, condition of discontinuities, groundwater conditions, and the orientation of discontinuities. The final RMR value ranges from 0, representing very poor rock mass quality, to 100, indicating very good rock quality (see Table 2).

Table 2. Rock mass rating (RMR) classification. Adapted from [8,38].

RMR	100–81	80–61	60–41	40–21	<20
Class	I	II	III	IV	V
Rock quality	Very good	Good	Fair	Poor	Very poor

Over the years, the Q-system has been applied to the assessment of cave stability, with several contributions extending its use to natural underground cavities [37,40,41]. Waltham and Fookes [41] proposed that a cave may be considered stable when its roof thickness exceeds approximately 70% of the cave width. In contrast, the approach developed by Waltham [37] adopts a more comprehensive framework, incorporating external support conditions and modifying the original Q-span stability relationship introduced by Barton [42] (see Figure 6).

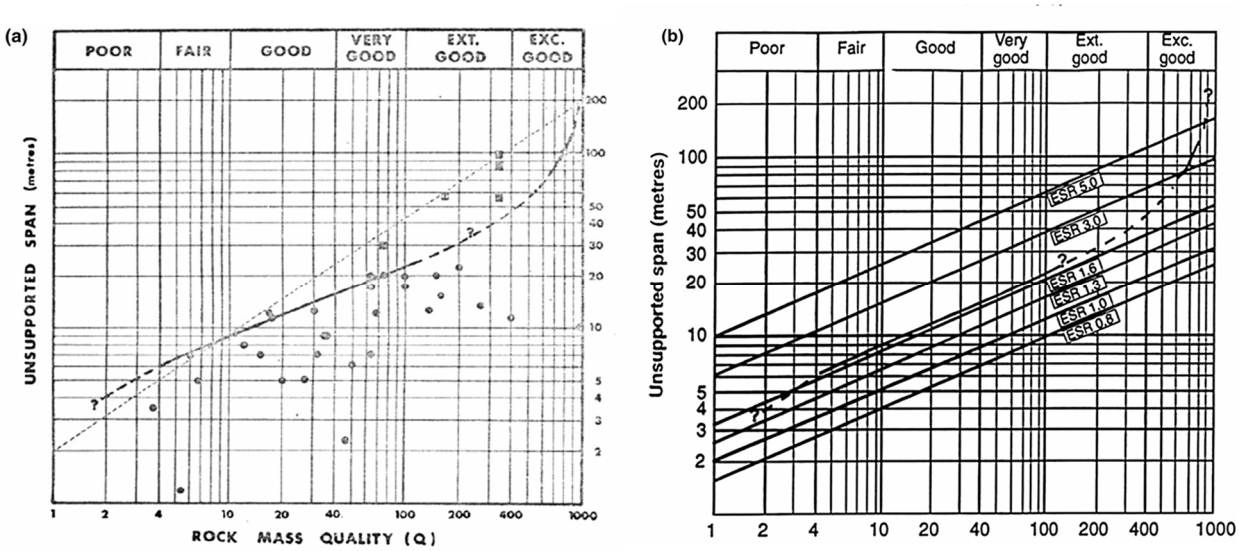

Figure 6. (**a**) Relationship between opening span and rock mass quality (Q index). Circles indicate unsupported man-made excavations, while squares correspond to natural cavities (Carlsbad Caverns, New Mexico). The curved envelope defines the upper limit for engineered openings, and the dashed line extends this limit to include natural caves. (**b**) ESR approach used to adjust the equivalent span according to excavation conditions [42].

In 2017, Jordá-Bordehore proposed a dedicated graphical framework for assessing the stability of natural caves [6]. This approach classifies underground cavities into three stability domains; however, in practice, the available case histories were mainly distributed within two dominant categories: stable and transitional conditions. The methodology was calibrated using an extensive dataset of more than one hundred caves developed across a wide range of lithological settings, providing a robust empirical basis for its application. The calibration results consistently showed that most cases fall within the stable and transitional fields, suggesting a strong clustering of natural caves within these stability domains and reinforcing the practical relevance of the proposed classification scheme [6] (see Figure 7).

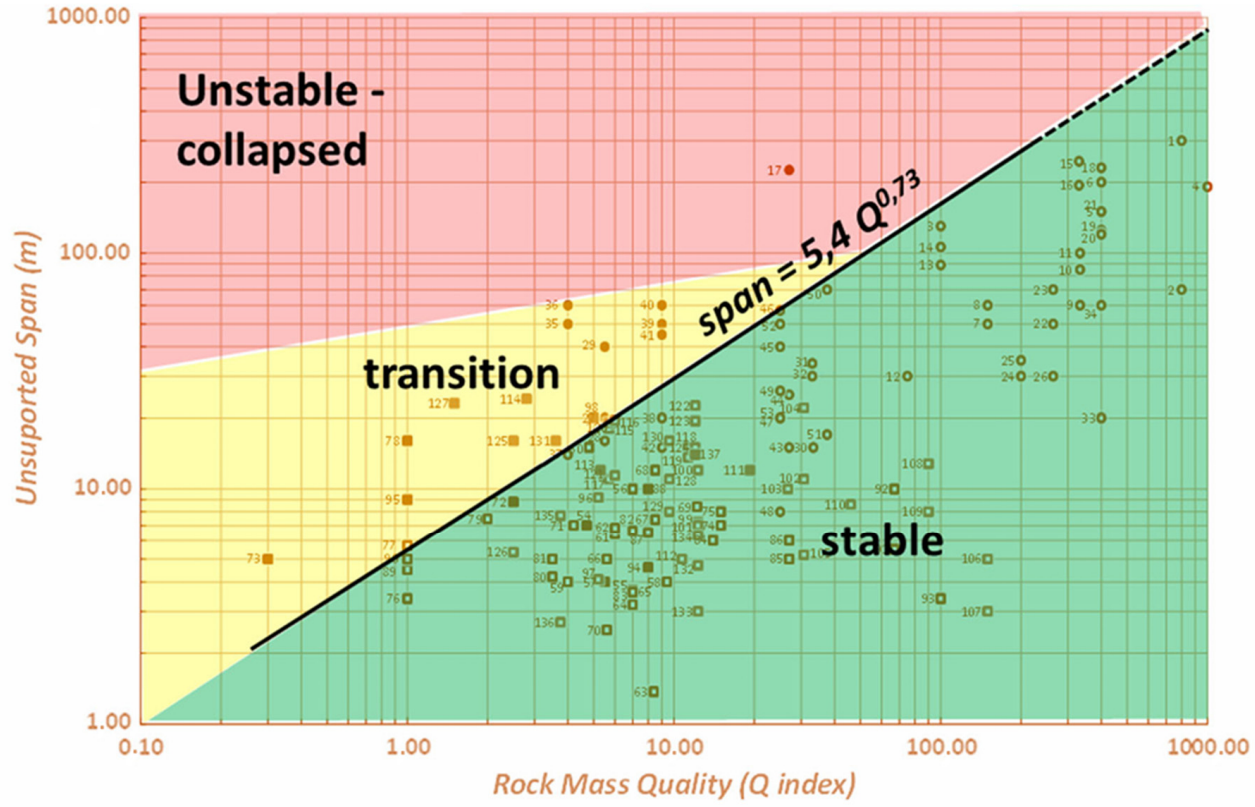

Figure 7. Q-span chart presented by Jorda (2017) [6].

3.2. The Scaled Span Method for the Stability of Crown Pillars

The Scaled Span Method is an empirical approach that was originally developed in Canada during the 1980s and has since become widely adopted as a primary tool for the preliminary assessment of crown pillar stability in surface and underground mining environments [10–12]. Beyond its original application, the method has also been extended to evaluate the rock mass between the ground surface and underground voids, including natural cave roofs [10–12,43].

This approach is based on the comparison between two key parameters: the critical span (Sc), which represents the maximum stable opening size under given rock mass conditions, and the scaled span (Cs), which incorporates both geometric and geomechanical characteristics of the excavation. The relationship between these parameters is used to estimate the stability condition of the crown pillar.

The safety factor F0S is defined as the ratio between the critical span and the scaled span, as proposed in previous studies by Carter and Miller [10–12]:

$$F0S = Sc/Cs$$

The scaled span of the crown pillar is defined as follows:

$$C_s = S\left\{\frac{y}{T[(1+S_r)(1-0.1\cos\theta)]}\right\}^{0.5}$$

where Cs is the scaled span expressed in meters, S represents the actual span of the excavation (m), y is the unit weight of the crown rock (g/cm^3), T is the thickness of the crown pillar (m), SR = S/L is the ratio between the span (or opening width) and the length of the mined area, and θ denotes the dip of the orebody or foliation. In situations involving

additional surface loading, such as lakes, soil cover, or infill materials, an equivalent effective density (y_eff) is considered instead of the rock unit weight [10–12].

Figure 8 illustrates the idealized geometry of a shallow volcanic cave and the key geometric parameters required for the calculation of the Scaled Span. A particular consideration concerns the parameter θ, which in mining applications originally represents the dip of the stope, typically associated with orebody orientation, vein geometry, or stratification planes.

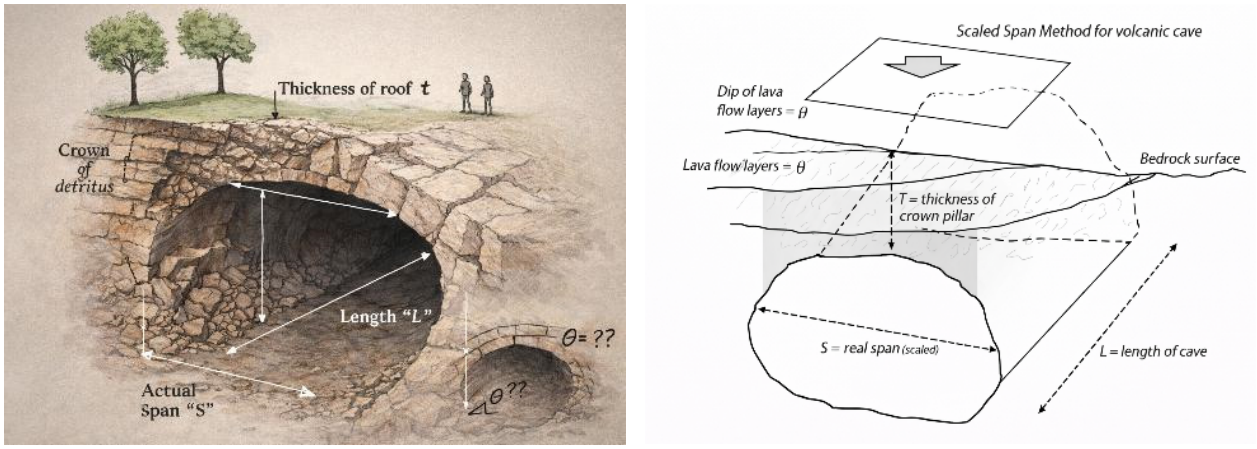

(**a**) (**b**)

Figure 8. (**a**) Scaled span approach applied to volcanic caves, illustrating the cave geometry and the main variables involved in its calculation. (**b**) Conceptual diagram of crown pillar conditions in natural cavities, outside a mining context [1].

In the context of natural caves, the definition of this parameter is less straightforward. If the cave geometry is assumed to be vertically developed, the value of θ = 90° could be considered. However, if θ is related to geological layering, such as stratification in limestone or basaltic sequences, a sub-horizontal orientation would often be more representative [1,13].

Additionally, adopting θ = 0° leads to cos θ = 1, which results in the maximum possible value of the Scaled Span (Cs). This condition corresponds to the most unfavorable scenario for stability assessment and therefore represents a conservative approach in the calculation [1,13].

The relationship used to express the probability of failure as a function of the safety factor is given as follows:

$$\mathrm{Pf}(\%) = \frac{100}{1 + 441\exp(-1.7\mathrm{C_s}/Q^{0.44})}$$

4. Results

Visual inspection of the studied lava tubes in Lanzarote, the Galápagos Islands, and Harrat al Shaam shows that instability mechanisms are mainly associated with a limited number of recurrent processes that are consistent across the investigated volcanic environments. The most frequent mechanism corresponds to localized detachment of rock slabs from the roof and sidewalls. This process is mainly controlled by the geometry and persistence of discontinuities, as well as the degree of fracturing of the basaltic rock mass. In most cases, these detachments are partial and do not result in complete structural failure of the cavity. Progressive block fall is commonly observed to stabilize after the formation of a natural load-transfer arch, which limits further collapse propagation into the interior of the lava tube [2,17,18,27]. This pattern is observed in well-preserved sections of caves in Lanzarote (e.g., Jameo hundido), where instability remains localized (Figure 5b).

A second mechanism is identified in shallow cavities where roof thickness is insufficient for arch formation. In these cases, progressive block detachment may evolve into surface collapse and sinkhole development. Due to the limited overburden, failure propagates toward the surface through a cascading or domino-like mechanism. This type of behavior is mainly observed in entrance zones or areas close to the ground surface, where higher joint density and tensile stress concentration in the roof are present. A similar response is observed in Harrat al Shaam, particularly within more fractured basaltic units. In cases where cavities are located at shallow depth or affected by dense discontinuity networks, transition from localized failure to surface collapse is also observed.

4.1. Q Index Determination

Table 3 presents the results obtained for the Q index for each of the analyzed caves. Likewise, it includes the main geomechanical parameters used in this classification, among which are the Rock Quality Designation (RQD), the number of joint sets (Jn), the joint roughness number (Jr), the joint alteration number (Ja), the water reduction factor (Jw), and the stress reduction factor of the rock mass (SRF).

To support the stability assessment of the studied caves, the results obtained from the Q-system analysis are presented graphically in Figure 9, allowing a more comprehensive and comparative evaluation of the rock mass conditions across the different sites.

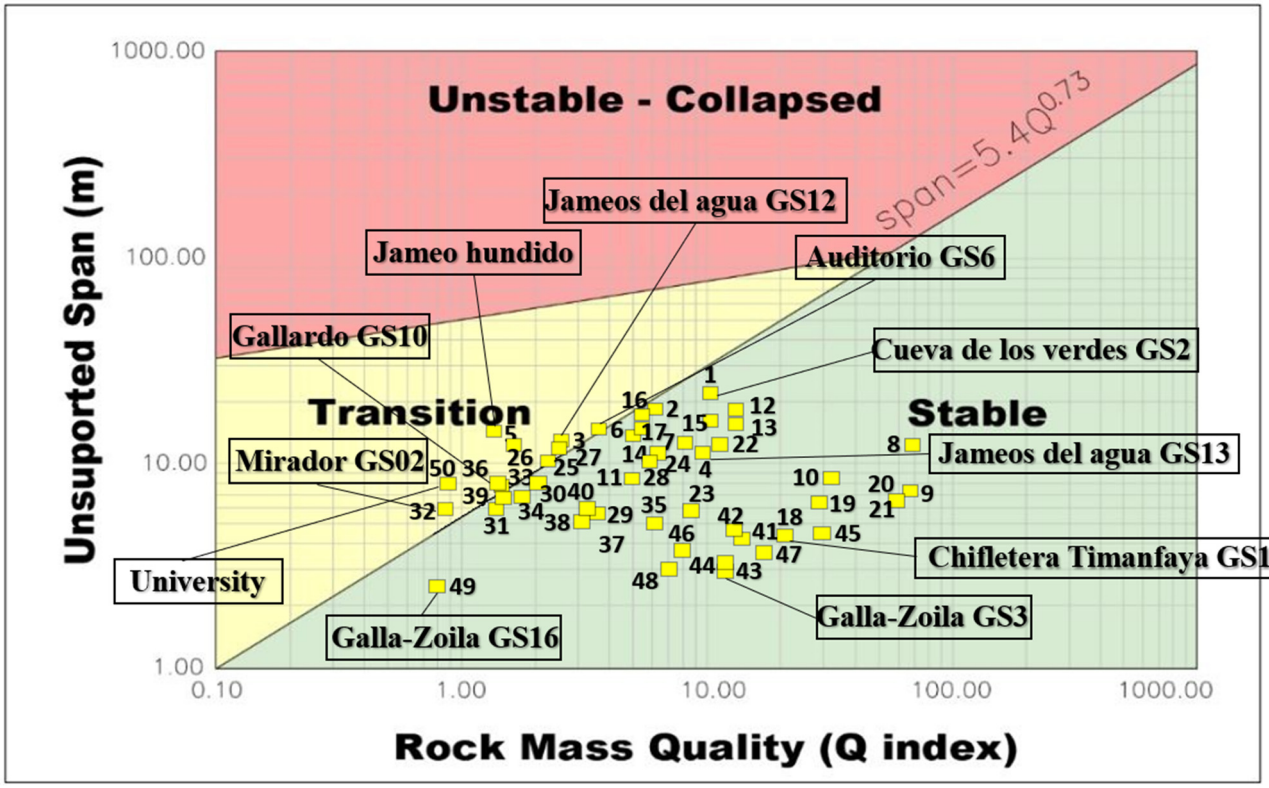

Figure 9. Stability classification of the studied caves based on the Q-system chart, adapted from [6].

Table 3. Geomechanical parameters used for the Q-system classification and geometric characteristics of the studied caves.

Location		Dimensions			Rock Mass Quality Q Index								Visual Observation	Code
Country	**Cave**	**Width (m)**	**Span Length (m)**	**Ceiling Thickness (m)**	**RQD**	**Jn**	**Jr**	**Ja**	**Jw**	**SRF**	**Q**	**RMR**		
Lanzarote Canarias, Spain	Cueva de los verdes GS2	23	100	4	92	9	3	1	1	2.5	12.2	/	Stable	1
	Jameo de La puerta falsa GS9	19.5	50	3.5	90	9	3	1	1	5	6	/	Minor Instabilities	2
	Jameos del agua GS12	16	20	2	75	9	3	2	1	5	2.5	/	Unstable	3
	Jameos del agua GS13	11	50	8.5	72	9	3	1	1	2.5	9.6	/	Minor Instabilities	4
	Jameo hundido	15	23	2	75	15	3	2	1	5	1.5	/	Unstable	5
	Auditorio GS15	16	43	2–10	72	12	3	1	1	2.5	3.6	/	Minor Instabilities	6
	Cueva de los verdes entrada	12	30	4	92	9	3	1	1	2.5	12.3	/	Stable	7
	Cueva de los verdes auditorio	12.8	30	4	90	3	3	1	1	1	90	/	Stable	8
	Cueva de los verdes auditorio	8	30	4.5	90	3	3	1	1	1	90	/	Stable	9
	Cueva de los verdes laborat	8	25	4.5	92	6	3	1	1	1	46	/	Stable	10
	Cueva de los verdes salida	9	50	4	78	9	3	1	1	5	5	/	Stable	11
	Jameo de La puerta falsa GS10	22	22	3.5	90	9	3	1	1	2.5	12	/	Stable	12
	Jameo de La puerta falsa GS11	19	20	4	90	9	3	1	1	2.5	12	/	Stable	13
	Jameo de La puerta falsa GS12	16	25	4	75	9	3	2	1	2.5	5	/	Stable	14
	Jameo de La puerta falsa GS13	15	25	3.5	90	9	3	1	1	2.5	12	/	Stable	15
	Jameo de La puerta falsa ZS	19	20	3.5	90	9	3	1	1	5	6	/	Stable	16
	Jameos del agua auditorio	16	20	8	82	12	3	2	1	2.5	6	/	Stable	17
	Chifletera Timanfaya GS16	4.7	15	4	92	3	4	4	1	2.5	12	/	Stable	18
	Chifletera Timanfaya GS17	6	15	4	92	3	4	4	1	2.5	12	/	Stable	19
	Playa del Paso Timanfaya GS18	7	10	3.5	75	2 × 3	3	2	1	5	75	/	Stable	20
	Playa del Paso Timanfaya GS19	7	10	4	75	2 × 3	3	2	1	5	75	/	Stable	21
	Playa del Paso Timanfaya GS20	14	20	4	90	9	3	1	1	5	12	/	Stable	22
	Jameo 7 lagos GS3	5	10	3	80	9	3	1	1	2.5	10	/	Stable	23
	Jameo 7 lagos GS4	12	15	3	80	9	3	1	1	5	5	/	Stable	24
Jordan	Al Badia Cave GS1	12	90	8	80	9	3	4	1	2.5	2.7	49	Stable	25
	Al Badia Cave GS2	16	120	5	95	15	3	2	1	5	1.9	58	Stable	26
	Al Badia Cave GS3	16	120	4	80	9	3	2	1	5	2.7	60	Unstable	27
	Dhadal Cave	8.8	16	1	95	9	3	1	1	5	6.4	66	Unstable	28
	Azzam Cave GS1	5.5	15	1.5	95	9 × 2	3	1	1	5	3.2	73	Stable	29
	Azzam Cave GS2	8	15	2	95	9	3	1	1	5	6.4	71	Stable	30

Table 3. *Cont.*

Location		Dimensions			Rock Mass Quality Q Index								Visual Observation	Code
Country	**Cave**	**Width (m)**	**Span Length (m)**	**Ceiling Thickness (m)**	**RQD**	**Jn**	**Jr**	**Ja**	**Jw**	**SRF**	**Q**	**RMR**		
Galapagos, Ecuador	Mirador GS-M-01	6.4	19	1	78	2 × 9	3	2	1	5	1.3	57	Stable	31
	Mirador GS-M-02	6.3	19	3.6	50	2 × 9	3	2	1	5	0.83	64	Stable	32
	Mirador GS-M-04	8.4	24.8	1.5	90	2 × 9	3	2	1	5	1.5	62	Stable	33
	Mirador GS-M-05	7	48	1	80	2 × 9	3	2	1	5	1.78	53	Stable	34
	Gallardo GS-G-05	5	47	10	75	9	3	4	1	1	6.25	43	Stable	35
	Gallardo GS-G-10	8.5	55	5.6	100	9	3	4	1	1	1.67	50	Unstable	36
	Gallardo GS-G-12	4.8	40	5.6	100	9	3	4	1	5	3.33	52	Stable	37
	Gallardo GS-G-14	6.5	80	5.3	95	9	3	4	1	2.5	3.17	57	Stable	38
	Gallardo GS-G-15	7	40	2	95	2 × 9	3	2	1	5	1.58	61	Minor Instabilities	39
	Gallardo GS-G-12b	6	40	5.6	100	9	3	4	1	2.5	3.33	52	Stable	40
	Galla-Zoila GS-GZ-01	4.3	40	14.6	85	9	3	2	1	1	14.2	59	Stable	41
	Galla-Zoila GS-GZ-02	4.8	40	14.7	80	9	3	2	1	1	13.33	59	Stable	42
	Galla-Zoila GS-GZ-03	2.7	40	18.8	75	9	3	2	1	1	12.5	58	Stable	43
	Galla-Zoila GS-GZ-04	3.2	40	15.2	75	9	3	2	1	1	12.5	62	Stable	44
	Galla-Zoila GS-GZ-08	4.5	40	13.1	100	9	3	1	1	1	33.33	56	Minor Instabilities	45
	Galla-Zoila GS-GZ-11	3.7	10	9.9	75	9	3	3	1	1	8.33	53	Minor Instabilities	46
	Galla-Zoila GS-GZ-13	3.6	30	11.4	100	9	3	2	1	1	17	69	Stable	47
	Galla-Zoila GS-GZ-15	3.1	40	2.6	100	9	3	2	1	1	7	69	Stable	48
	Galla-Zoila GS-GZ-16	2.57	40	3.5	50	2 × 9	3	4	1	2.5	0.83	46	Stable	49
	University Cave, Main Room	8	7.5	2	74	3 × 6	1	1	1	5	2	55	Unstable	50

4.2. Stability Assessment Using the Scaled Span Method

The Scaled Span Method has been applied to all the studied caves in order to evaluate their potential for instability, particularly in relation to failure mechanisms that may propagate towards the ground surface. Although the original formulation of the stability graph was developed for underground mining environments, previous studies have demonstrated its applicability to shallow natural cavities, including lava tubes [1].

For the present analysis, the required geometric and geomechanical input parameters, including span dimensions and rock mass quality values, were extracted from Table 3. Each cave was subsequently evaluated following the methodology described in Section 3, and the corresponding calculated parameters and results are summarized in Table 4.

The results of the Scaled Span analysis, which evaluate the stability of the rock mass between the cave roof and the ground surface, are presented graphically using a modified stability chart based on the original framework proposed by Carter (2014) [12]. In this representation, stability is expressed as a function of the Scaled Span and the rock mass quality (Q), as shown in Figure 10.

Table 4. Determination of approximate values of the scaled span index.

Location		Dimensions						Code
Country	**Cave**	**Width (m)**	**Span Length (m)**	**Ceiling Thickness (m)**	**Q**	**Cs Scaled Span (m)**	**Probability of Failure %**	
Lanzarote Canarias, Spain	Cueva de los verdes GS2	23	100	4	12.2	17.35	70%	1
	Jameo de La puerta falsa GS9	19.5	50	3.5	6	14.79	75%	2
	Jameos del agua GS12	16	20	2	2.5	14.11	90%	3
	Jameos del agua GS13	11	50	8.5	9.6	5.72	8%	4
	Jameo hundido	15	23	2	1.5	13.81	100%	5
	Auditorio GS15	16	43	2–10	3.6	10.22	70%	6
	Cueva de los verdes entrada	12	30	4	12.3	8.49	22%	7
	Cueva de los verdes auditorio	12.8	30	4	90	8.97	1.6%	8
	Cueva de los verdes auditorio	8	30	4.5	90	5.56	0.6%	9
	Cueva de los verdes laborat	8	25	4.5	46	5.44	1%	10
	Cueva de los verdes salida	9	50	4	5	6.93	50%	11
	Jameo de La puerta falsa GS10	22	22	3.5	12	13.91	55%	12
	Jameo de La puerta falsa GS11	19	20	4	12	11.38	51%	13
	Jameo de La puerta falsa GS12	16	25	4	5	10.45	60%	14
	Jameo de La puerta falsa GS13	15	25	3.5	12	10.61	50%	15
	Jameo de La puerta falsa ZS	19	20	3.5	6	12.17	60%	16
	Jameos del agua auditorio	16	20	8	6	7.06	35%	17
	Chifletera Timanfaya GS16	4.7	15	4	12	3.43	1.5%	18
	Chifletera Timanfaya GS17	6	14	4	12	4.2	3%	19
	Playa del Paso Timanfaya GS18	7	10	3.5	75	4.8	0.6%	20
	Playa del Paso Timanfaya GS19	7	10	4	75	4.49	0.5%	21
	Playa del Paso Timanfaya GS20	14	20	4	12	8.98	35%	22
	Jameo 7 lagos GS3	5	10	3	10	3.94	3%	23
	Jameo 7 lagos GS4	12	15	3	5	8.64	55%	24
Jordan	Al Badia Cave GS1	12	90	8	2.7	6.67	55%	25
	Al Badia Cave GS1	16	120	5	1.9	11.25	90%	26
	Al Badia Cave GS1	16	120	4	2.7	12.57	80%	27
	Dhadal Cave	8.8	16	1	6.4	11.83	60%	28
	Azzam Cave GS1	5.5	15	1.5	3.2	6.43	52%	29
	Azzam Cave Gs2	8	15	2	6.4	7.64	49%	30

Table 4. *Cont.*

Location		Dimensions						Code
Country	**Cave**	**Width (m)**	**Span Length (m)**	**Ceiling Thickness (m)**	**Q**	**Cs Scaled Span (m)**	**Probability of Failure %**	
Galapagos, Ecuador	Mirador GS-M-01	6.4	19	1	1.3	9.27	75%	31
	Mirador GS-M-02	6.3	19	3.6	0.83	4.81	55%	32
	Mirador GS-M-04	8.4	24.8	1.5	1.5	9.92	70%	33
	Mirador GS-M-05	7	48	1	1.78	10.94	70%	34
	Gallardo GS-G-05	5	47	10	6.25	2.52	1.5%	35
	Gallardo GS-G-10	8.5	55	5.6	1.67	5.59	60%	36
	Gallardo GS-G-12	4.8	40	5.6	3.33	3.21	5%	37
	Gallardo GS-G-14	6.5	80	5.3	3.17	4.51	20%	38
	Gallardo GS-G-15	7	40	2	1.58	7.64	60%	39
	Gallardo GS-G-12b	6	40	5.6	3.33	3.96	11%	40
	Galla-Zoila GS-GZ-01	4.3	40	14.6	14.2	1.91	0.1%	41
	Galla-Zoila GS-GZ-02	4.8	40	14.7	13.33	1.99	0.5%	42
	Galla-Zoila GS-GZ-03	2.7	40	18.8	12.5	1.01	0%	43
	Galla-Zoila GS-GZ-04	3.2	40	15.2	12.5	1.32	0%	44
	Galla-Zoila GS-GZ-08	4.5	40	13.1	33.33	1.73	0%	45
	Galla-Zoila GS-GZ-11	3.7	10	9.9	8.33	1.86	0.8%	46
	Galla-Zoila GS-GZ-13	3.6	30	11.4	17	1.71	0%	47
	Galla-Zoila GS-GZ-15	3.1	40	2.6	7	3.1	2%	48
	Galla-Zoila GS-GZ-16	2.57	40	3.5	0.83	2.23	5%	49
	University Cave, Main Room	8	7.5	2	2	6.58	25%	50

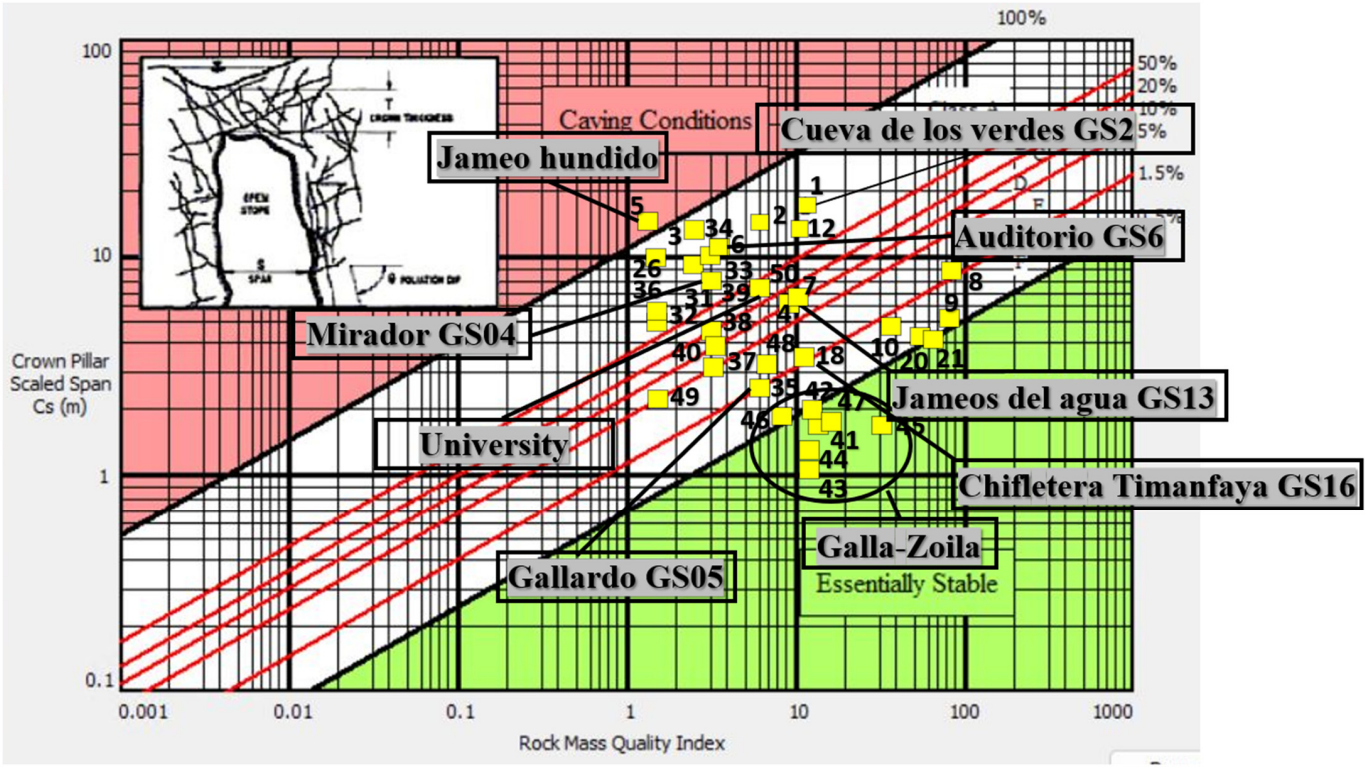

Figure 10. Crown pillar stability chart expressed in terms of Scaled Span and rock mass quality (Q), adapted from [12].

Table 5 provides a comparative overview of the different approaches used to assess cave stability, including the Q-system, the Scaled Span Method, and direct visual observations carried out in the field. This comparison aims to evaluate the consistency between

empirical classifications, geometric-based methods, and observed structural behavior of the lava tubes. By integrating these complementary approaches, it is possible to identify agreements and discrepancies in the predicted stability conditions, thereby improving the overall reliability of interpretation. The comparison also allows a more comprehensive understanding of how rock mass quality and geometric factors jointly control the stability of the studied caves.

Table 5. Determination of approximate values of the scaled span.

Location		Dimensions			Code
Country	**Cave**	**Visual Observation**	**Q—Span Graph**	**Scaled Span**	
Lanzarote Canarias, Spain	Cueva de los verdes GS2	Stable	Stable	Transition/Unstable	1
	Jameo de La puerta falsa GS9	Minor Instabilities	Stable	Transition/Unstable	2
	Jameos del agua GS12	Unstable	Transition	Transition/Unstable	3
	Jameos del agua GS13	Minor Instabilities	Stable	Transition/Stable	4
	Jameo hundido	Unstable	Transition	Unstable/Collapsed	5
	Auditorio GS15	Minor Instabilities	Transition	Transition/Unstable	6
	Cueva de los verdes entrada	Stable	Stable	Transition/Unstable	7
	Cueva de los verdes auditorio	Stable	Stable	Stable	8
	Cueva de los verdes auditorio	Stable	Stable	Stable	9
	Cueva de los verdes laborat	Stable	Stable	Stable	10
	Cueva de los verdes salida	Stable	Stable	Transition/Unstable	11
	Jameo de La puerta falsa GS10	Stable	Stable	Transition/Unstable	12
	Jameo de La puerta falsa GS11	Stable	Stable	Transition/Unstable	13
	Jameo de La puerta falsa GS12	Minor Instabilities	Transition	Transition/Unstable	14
	Jameo de La puerta falsa GS13	Stable	Stable	Transition/Unstable	15
	Jameo de La puerta falsa ZS	Stable	Transition	Transition/Unstable	16
	Jameos del agua auditorio	Stable	Stable	Transition/Unstable	17
	Chifletera Timanfaya GS16	Stable	Stable	Stable	18
	Chifletera Timanfaya GS17	Stable	Stable	Stable	19
	Playa del Paso Timanfaya GS18	Stable	Stable	Stable	20
	Playa del Paso Timanfaya GS19	Stable	Stable	Stable	21
	Playa del Paso Timanfaya GS20	Stable	Stable	Transition/Unstable	22
	Jameo 7 lagos GS3	Stable	Stable	Transition/Stable	23
	Jameo 7 lagos GS4	Stable	Stable	Transition/Unstable	24
Jordan	Al Badia Cave GS1	Stable	Transition	Transition/Unstable	25
	Al Badia Cave GS1	Stable	Transition	Transition/Unstable	26
	Al Badia Cave GS1	Unstable	Transition	Transition/Unstable	27
	Dhadal Cave	Stable	Stable	Transition/Unstable	28
	Azzam Cave GS1	Stable	Stable	Transition/Unstable	29
	Azzam Cave Gs2	Stable	Stable	Transition/Unstable	30
Galapagos, Ecuador	Mirador GS-M-01	Stable	Stable	Transition/Unstable	31
	Mirador GS-M-02	Stable	Transition	Transition/Unstable	32
	Mirador GS-M-04	Stable	Stable	Transition/Unstable	33
	Mirador GS-M-05	Stable	Stable	Transition/Unstable	34
	Gallardo GS-G-05	Stable	Stable	Transition/Stable	35
	Gallardo GS-G-10	Unstable	Transition	Transition/Unstable	36
	Gallardo GS-G-12	Stable	Stable	Transition/Stable	37
	Gallardo GS-G-14	Stable	Stable	Transition/Stable	38
	Gallardo GS-G-15	Minor Instabilities	Stable	Transition/Unstable	39
	Gallardo GS-G-12b	Stable	Stable	Transition/Stable	40
	Galla-Zoila GS-GZ-01	Stable	Stable	Stable	41
	Galla-Zoila GS-GZ-02	Stable	Stable	Stable	42
	Galla-Zoila GS-GZ-03	Stable	Stable	Stable	43
	Galla-Zoila GS-GZ-04	Stable	Stable	Stable	44
	Galla-Zoila GS-GZ-08	Minor Instabilities	Stable	Stable	45
	Galla-Zoila GS-GZ-11	Minor Instabilities	Stable	Stable	46
	Galla-Zoila GS-GZ-13	Stable	Stable	Stable	47
	Galla-Zoila GS-GZ-15	Stable	Stable	Transition/Stable	48
	Galla-Zoila GS-GZ-16	Stable	Stable	Transition/Stable	49
	University Cave, Main Room	Unstable	Transition	Transition/Unstable	50

5. Discussion

The comparison between the different stability assessment approaches reveals an overall general consistency in the identification of stable and unstable conditions across the studied lava caves. In many cases, the three approaches—visual inspection, Q-system classification, and Scaled Span analysis—converge towards similar stability interpretations, particularly for caves exhibiting well-developed rock mass conditions or clearly degraded structural zones. For example, caves such as Galla-Zoila, Chifletera Timanfaya and Cueva de los verdes auditorio, are consistently classified as stable, whereas Jameo hundido is identified as unstable or partially collapsed across the applied methodologies.

However, important discrepancies arise when comparing the Q-system results with those obtained from the Scaled Span Method. As illustrated in Figure 10, several caves (e.g., 1, 2, 3, 4, and 6) plot near or within the transition to failure domain in the Scaled Span chart, indicating a relatively high probability of instability. In contrast, the Q-system classification places some of these same caves (e.g., 1, 2, and 4) within stable conditions (Figure 9). This divergence suggests that the two approaches may respond differently to the geometric sensitivity of shallow cavities, particularly with respect to roof thickness and span, which are explicitly incorporated in the Scaled Span formulation but only indirectly represented in the Q-system.

In several cases, the observed instability is limited to localised zones rather than global structural failure, which may explain part of the discrepancy between methods. Minor detachments and localized block falls are observed in caves classified as stable by the Q-system but positioned closer to the failure threshold in the Scaled Span chart. This highlights that empirical classifications based solely on rock mass quality may not fully capture geometric controls governing shallow cave stability [1,4,26].

It is important to emphasize that both methods should be interpreted as preliminary screening tools rather than definitive stability analyses. Their main value lies in providing a first-order approximation of potential instability conditions and supporting decision-making in reconnaissance-level studies. In all cases, a "stable" classification does not imply the absence of local rock falls or slab detachments, which may still pose significant hazards, particularly in tourist-accessible caves [6,12,42]. For this reason, detailed site-specific analyses and stabilization measures are required in critical zones, including the use of rock bolting or other reinforcement techniques where necessary.

A further limitation concerns the original development context of the Scaled Span Method, which was designed for crown pillar assessment in mining environments. Its application to natural lava tubes introduces additional uncertainties, particularly regarding geometry irregularities, heterogeneous rock mass conditions, and differences in failure mechanisms compared to engineered excavations [12]. Therefore, caution is required when directly transferring mining-based empirical relationships to volcanic cave systems.

Overall, the combined use of Q-system classification and Scaled Span analysis provides a more robust framework for evaluating shallow cave stability than either method alone. While the Q-system captures rock mass quality, the Scaled Span Method introduces a stronger geometric control, making their integration particularly useful for identifying potentially critical conditions in volcanic caves [1,4].

6. Conclusions

This study assessed the stability of volcanic lava tubes located in different geological settings, including the Canary Islands, the Galápagos archipelago, and the Harrat al Shaam lava field. The analysis combined field observations with two approaches for rock mass stability assessment—the Q-system and the Scaled Span Method

(SSM)—allowing a comparative evaluation of empirical and geometry-based methods in shallow volcanic caves.

The results indicate that rock mass classification tools such as the Q-system, together with span-based approaches, provide a useful first-order indication of cave stability based on rock mass quality. However, their predictive capability is limited when it comes to capturing specific geometric controls, such as roof thickness and span variations, which are critical in shallow underground cavities.

The SSM, which extends the Q-system by incorporating geometric scaling factors, shows improved sensitivity to conditions typical of shallow caves. However, its original formulation for mining crown pillar design introduces limitations when applied directly to natural volcanic systems, where boundary conditions, heterogeneity, and geological evolution differ significantly.

Overall, differences between the two methods are mainly observed in cases where localised instability does not necessarily imply global collapse, but rather reflects structurally controlled detachments or limited roof failures.

The combination of the Q-system and SSM therefore provides a more complete preliminary framework for assessing lava tube stability. Nevertheless, both approaches should be considered as screening tools that require site-specific analysis for more robust hazard evaluation, particularly in caves located near infrastructure or used for tourism.

Future work will focus on expanding the dataset to include additional volcanic caves, improving the robustness of the comparisons, and further exploring relationships between empirical rock mass classifications and geometry-based stability approaches.

Author Contributions: Conceptualization, L.J.-B. and A.B.; methodology, A.B., S.S.D. and L.J.-B.; software, A.B. and S.S.D.; validation, L.J.-B.; formal analysis, S.S.D. and L.J.-B.; investigation, A.B. and L.J.-B.; resources, A.B., S.S.D. and L.J.-B.; data curation, A.B. and L.J.-B.; writing—original draft preparation, A.B. and L.J.-B.; writing—review and editing, S.S.D.; visualization, A.B.; supervision, S.S.D. and L.J.-B.; project administration, L.J.-B. and S.S.D. All authors have read and agreed to the published version of the manuscript.

Funding: This research was funded by UPM Technical University of Madrid grant number RP2504350220 "Geotecnia sin fronteras—geotechnics without borders".

Data Availability Statement: The original contributions presented in this study are included in the article. Further inquiries can be directed to the corresponding author.

Conflicts of Interest: The authors declare no conflicts of interest.

References

1. Jordá-Bordehore, L.; Toulkeridis, T.; Romero-Crespo, P.L.; Jordá-Bordehore, R.; Garizábal, I.G. Stability assessment of volcanic lava tubes in the Galápagos using engineering rock mass classifications and an empirical approach. *Int. J. Rock Mech. Min. Sci.* **2016**, *89*, 55–67. [CrossRef]
2. Bastidas, G.; Soria, O.; Mulas, M.; Loaiza, S.; Bordehore, L.J. Stability Analysis of Lava Tunnels on Santa Cruz Island (Galapagos Islands, Ecuador) Using Rock Mass Classifications: Empirical Ap-proach and Numerical Modeling. *Geosciences* **2022**, *12*, 380. [CrossRef]
3. Rodríguez, G.; Mulas, M.; Loaiza, S.; Echeverria, M.D.P.V.; Yanez Vinueza, A.A.; Larreta, E.; Jordá Bordehore, L. Stability Analysis of the Volcanic Cave El Mirador (Galápagos Islands, Ecuador) Combining Numerical, Empirical and Remote Techniques. *Remote Sens.* **2023**, *15*, 732. [CrossRef]
4. Herrera, R.; Garcés, D.; Benrabah, A.; Al-Malabeh, A.; Jordá-Bordehore, R.; Jordá-Bordehore, L. State of the Art on Empirical and Numerical Methods for Cave Stability Analysis: Application in Al-Badia Lava Tube, Harrat Al-Shaam, Jordan. *Appl. Mech.* **2025**, *6*, 56. [CrossRef]

5. Jordá-Bordehore, L.; Al-Malabeh, A.; Abdelmadjid, B.; Jordá-Bordehore, R. Discusión sobre la aplicabilidad de metodologías empíricas "tuneleras" para análisis de estabilidad de cuevas: Caso del tubo de lava de Al-Badia, en Harrat Al-Shaam, Jordania. In Proceedings of the IX Congreso Español Sobre Cuevas y Minas Turísticas, Geología y Turismo: Realidades Complementarias, Karrantza, Spain, 22–25 October 2024; pp. 229–239.
6. Jordà-Bordehore, L. Stability Assessment of Natural Caves Using Empirical Approaches and Rock Mass Classifications. *Rock Mech. Rock Eng.* **2017**, *50*, 2143–2154. [CrossRef]
7. Benrabah, A.; Domínguez, S.S.; Bordehore, L.J.; Alonzo, D.A.; Herrero, A.D.; de Andrés Herrero, M. Preliminary Assessment of Badajo Cave (Segovia, Spain) Stability Using Empirical, Numerical and Remote Techniques. *IOP Conf. Ser. Earth Environ. Sci.* **2024**, *1295*, 012011. [CrossRef]
8. Benrabah, A.; Senent Domínguez, S.; Collado Giraldo, H.; Chaves Rodríguez, C.; Jorda Bordehore, L. Stability Assessment of the Maltravieso Cave (Caceres, Spain) Through Engineering Rock Mass Classification, Empirical, Numerical and Remote Techniques. *Remote Sens.* **2024**, *16*, 3883. [CrossRef]
9. Jordà-Bordehore, L.; García, R.; Alonso-Zarza, A.; Romero, C. Stability assessment of shallow limestone caves through an empirical approach: Application of the stability graph method to the Castañar Cave study site (Spain). *Bull. Eng. Geol. Environ.* **2016**, *75*, 1469–1483. [CrossRef]
10. Carter, T.G.; Miller, R.I. Crown-pillar risk assessment-planning aid for cost-effective mine closure remediation. *Trans. Inst. Min. Metall.* **1995**, *104*, 41–57.
11. Carter, T.; Cottrell, B.E.; Carvalho, J.; Steed, C. Logistic Regression improvements to the Scaled Span Method for dimensioning Surface Crown Pillars over Civil or Mining Openings. In Proceedings of the 42nd US Rock Mechanics Symposium and 2nd Can-US Rock Mechanics Symposium, San Francisco, CA, USA, 29 June–2 July 2008; p. ARMA-08-282.
12. Carter, T. Guidelines for use of the Scaled Span Method for Surface Crown Pillar Stability Assessment. In Proceedings of the 1st International Conference on Applied Empirical Design Methods in Mining, Lima, Peru, 9 June 2014.
13. Benrabah, A.; Senent, S.; Jorda-Bordehore, L. Application of the scaled span method for stability analysis of volcanic caves. In *New Challenges in Rock Mechanics and Rock Engineering*; CRC Press: Boca Raton, FL, USA, 2024; pp. 388–394.
14. Carracedo, J.C.; Day, S.; Guillou, H.; Pérez Torrado, F.J. Hotspot volcanism close to a passive continental margin: The Canary Islands. *Geol. Soc. Am. Bull.* **2002**, *114*, 1407–1426.
15. Troll, V.R.; Carracedo, J.C. The Canary Islands: An overview of their geology, evolution and volcanism. *Earth-Sci. Rev.* **2016**, *160*, 1–47. [CrossRef]
16. Carracedo, J.C.; Troll, V.R. *The Geology of the Canary Islands*; Elsevier: Amsterdam, The Netherlands, 2021.
17. Romero, C.; Guillou, H.; Carracedo, J.C.; Pérez Torrado, F.J. Volcanic hazard assessment of the Canary Islands. *Nat. Hazards* **2006**, *38*, 371–392.
18. Pedrazzi, D.; Becerril, L.; Martí, J.; Meletlidis, S.; Galindo, I. Explosive activity in basaltic systems: Insights from the Canary Islands. *J. Volcanol. Geotherm. Res.* **2013**, *257*, 21–38.
19. Pinkerton, H.; Wilson, L. Factors controlling the lengths of channel-fed lava flows. *Bull. Volcanol.* **1994**, *56*, 108–120. [CrossRef]
20. Calvari, S.; Pinkerton, H. Formation of lava tubes and extensive flow fields. *Bull. Volcanol.* **1998**, *59*, 291–303.
21. Calvari, S.; Ganci, G.; Galindo, I.; Sanz-Mangas, D.; Morgavi, D.; Lorenzo, O.F. Emplacement and growth of a stacked tube-fed lava flow field: The 2021 Tajogaite eruption (La Palma, Canary Islands, Spain). *Bull. Volcanol.* **2026**, *88*, 8. [CrossRef]
22. Bieniawski, Z.T. Engineering Classification of jointed rock Masses. *Trans. S. Afr. Inst. Civ. Eng.* **1973**, *15*, 335–344.
23. Barton, N.; Grimstad, E. The Q-system following twenty years of application in NMT support selection. In Proceedings of the 43rd Geomechanic Colloquy, Salzburg, Austria, 24–26 March 1994; pp. 428–436.
24. Tihansky, A.B. *Sinkholes, Subsidence, and Related Hazards*; US Geological Survey Circular: Reston, VA, USA, 1999; p. 1182.
25. Waltham, T.; Bell, F.; Culshaw, M. *Sinkholes and Subsidence*; Springer: Berlin/Heidelberg, Germany, 2005.
26. Parise, M.; Gunn, J. Natural and anthropogenic hazards in karst areas. *Geol. Soc. Spec. Publ.* **2007**, *279*, 1–3. [CrossRef]
27. Al-Malabeh, A. Geochemistry of Two Volcanic Cones from the Intra- continental plateau Basalt of Harra El-Jabban, NE-Jordan. *Geochem. J.* **1994**, *28*, 542–558. [CrossRef]
28. Al-Malabeh, A.; Frehat, M.; Henschel, H.-V.; Kempe, S. Al-Fahda Cave (Jordan): The longest lava cave yet reported from the Arabian Plate. In Proceedings of the 12th International Symposium on Vulcanospeleology, Tepotzlán, Mexico, 2–7 July 2006; pp. 201–208.
29. Al-Malabeh, A.; Kempe, S. Jordanian lava caves an overview. In Proceedings of the 15th International Symposium on Vulcanospeleology, Zarka, Jordan, 15–22 March 2012; pp. 38–42.
30. Al-Malabeh, A.; Hamed, R. Enrichment of radon (222rn) concentration in Remah volcano, NE-Jordan. *Iraqi Geol. J.* **2020**, *53*, 58–70. [CrossRef]
31. Sauro, F.; Pozzobon, R.; Massironi, M.; De Berardinis, P.; Santagata, T.; De Waele, J. Lava tubes on Earth, Moon and Mars: A review on their size and morphology revealed by comparative planetology. *Earth-Sci. Rev.* **2020**, *209*, 103288. [CrossRef]

32. Huerta, P.; Martín-Pérez, A.; Martín-García, R.; Rodríguez-Berriguete, Á.; La Iglesia Fernández, Á.; Alonso-Zarza, A.M. Gypsum speleothems in lava tubes from Lanzarote (Canary Islands): Ion sources and pathways. *Sediment. Geol.* **2019**, *383*, 136–147. [CrossRef]
33. Hoek, E.; Brown, E.T. Practical estimates of rock mass strength. *Int. J. Rock Mech. Min. Sci.* **1997**, *34*, 1165–1186. [CrossRef]
34. Parise, M. Engineering geology in karst. *Environ. Earth Sci.* **2015**, *74*, 7823–7837. [CrossRef]
35. Gutiérrez, F.; Parise, M.; De Waele, J.; Jourde, H. A review on natural and human-induced geohazards and impacts in karst. *Earth-Sci. Rev.* **2014**, *138*, 61–88. [CrossRef]
36. Rocscience. *Cpillar Software*, Rocscience: Toronto, ON, Canada, 2019. Available online: https://www.rocscience.com/software/cpillar (accessed on 12 June 2026).
37. Waltham, T. The Engineering Classification of Karst with Respect to the Role And Influence of Caves. *Int. J. Speleol.* **2002**, *31*, 19–35. [CrossRef]
38. Barton, N.; Bieniawski, Z. RMR and Q-setting records straight. *Tunn. Tunn. Int.* **2008**, *2*, 26–29.
39. Barton, N.; Lien, R.; Lunde, J. Enginnering Classification of Rock Masses for the Design of Tunnel Support. *Rock Mech. Rock Eng.* **1974**, *6*, 189–236. [CrossRef]
40. Barton, N.R.; Bandis, S.C. Characterization and Modelling of the Shear Strength, Stiffness and Hydraulic Behaviour of Rock Joints for Engineering Purposes. In *Rock Mechanics and Engineering*; Feng, X.-T., Ed.; Taylor & Francis: Abingdon, UK, 2017; Volume 1, Chapter 1; pp. 3–40.
41. Waltham, A.C.; Fookes, P.G. Engineering Classification of Karst Ground Conditions. *Q. J. Eng. Geol. Hydrogeol.* **2003**, *36*, 101–118. [CrossRef]
42. Barton, N. Unsupported underground openings. In *Rock Mechanics Discussion Meeting*; Befo, Swedish Rock Mechanics: Stockholm, Sweden, 1976; pp. 61–94.
43. Golder Associates. *Crown Pillar Stability Back-Analysis*; Report 881-1739 to CANMET; Report No. 23440-8-9074/01-SQ; CANMET: Ottawa, ON, Canada, 1990; p. 90.

Disclaimer/Publisher's Note: The statements, opinions and data contained in all publications are solely those of the individual author(s) and contributor(s) and not of MDPI and/or the editor(s). MDPI and/or the editor(s) disclaim responsibility for any injury to people or property resulting from any ideas, methods, instructions or products referred to in the content.